Functional Contacts With a Range of Splicing Proteins Suggest a Central Role for Brr2p in the Dynamic Control of the Order of Events in Spliceosomes of *Saccharomyces cerevisiae*

Rob W. van Nues and Jean D. Beggs

Wellcome Trust Centre for Cell Biology, University of Edinburgh, Edinburgh EH9 3JR, United Kingdom

Manuscript received September 11, 2000
Accepted for publication December 22, 2000

ABSTRACT

Mapping of functional protein interactions will help in understanding conformational rearrangements that occur within large complexes like spliceosomes. Because the U5 snRNP plays a central role in pre-mRNA splicing, we undertook exhaustive two-hybrid screening with Brr2p, Prp8p, and other U5 snRNP-associated proteins. DExH-box protein Brr2p interacted specifically with five splicing factors: Prp8p, DEAH-box protein Prp16p, U1 snRNP protein Snp1p, second-step factor Slu7p, and U4/U6.U5 tri-snRNP protein Snu66p, which is required for splicing at low temperatures. Co-immunoprecipitation experiments confirmed direct or indirect interactions of Prp16p, Prp8p, Snu66p, and Snp1p with Brr2p and led us to propose that Brr2p mediates the recruitment of Prp16p to the spliceosome. We provide evidence that the *prp8-1* allele disrupts an interaction with Brr2p, and we propose that Prp8p modulates U4/U6 snRNA duplex unwinding through another interaction with Brr2p. The interactions of Brr2p with a wide range of proteins suggest a particular function for the C-terminal half, bringing forward the hypothesis that, apart from U4/U6 duplex unwinding, Brr2p promotes other RNA rearrangements, acting synergistically with other spliceosomal proteins, including the structurally related Prp2p and Prp16p. Overall, these protein interaction studies shed light on how splicing factors regulate the order of events in the large spliceosome complex.

SPLICING of RNA is the removal of introns from messenger RNA precursors (pre-mRNAs) by two successive *trans*-esterification reactions. It is a highly dynamic process that is catalyzed by a multi-component complex, the spliceosome. During spliceosome formation and subsequent catalysis, conformational rearrangements of RNA-RNA, protein-protein, and protein-RNA interactions occur (reviewed in Staley and Guthrie 1998). The formation of a prespliceosomal complex is characterized by the ordered assembly of two small ribonucleoprotein (snRNP) particles, U1 and U2, on the pre-mRNA. U1 snRNA anneals to the intron at the junction with the first exon, the 5′ splice site. Mud2p and Msl5p are thought to direct the addition of the U2 snRNP (Abovich and Rosbash 1997; Fromont-Racine *et al.* 1997), which results in binding of U2 snRNA to the branchpoint sequence within the intron. Subsequent addition of the U4/U6.U5 tri-snRNP, preassembled from the U5 snRNP and the U4/U6 di-snRNP, is accompanied by rearrangements that lead to formation of the catalytic center needed for the first *trans*-esterification reaction.

During or just after U4/U6.U5 tri-snRNP recruitment to the prespliceosome the U4/U6 base pairing is disrupted by the U5 snRNP-associated RNA unwindase Brr2p (Slt22p/Snu246p/Rss1p/Prp44p; Lauber *et al.* 1996; Lin and Rossi 1996; Noble and Guthrie 1996; Xu *et al.* 1996; Kim and Rossi 1999) accompanied by ATP hydrolysis (Raghunathan and Guthrie 1998; Kim and Rossi 1999). Another U5 snRNP protein, Prp8p, that contacts U6 snRNA in U4/U6.U5 tri-snRNPs (Vidal *et al.* 1999) is proposed to regulate unwinding of the U4/U6 duplex (Kuhn *et al.* 1999) and to anchor the first exon in the spliceosome (Newman and Norman 1992; Teigelkamp *et al.* 1995; Dix *et al.* 1998). The rearranged U6 snRNA displaces U1 snRNA from the 5′ splice site in an ATP-dependent step facilitated by Prp28p (Staley and Guthrie 1999) and a more 3′ region of U6 snRNA binds to U2 snRNA to form the catalytic center of the spliceosome for the first step of splicing. Prp2p, an RNA-dependent NTPase like Brr2p, is required to activate the spliceosome but dissociates from it after ATP hydrolysis, when the first *trans*-esterification reaction takes place (Kim and Lin 1996).

Upon completion of the first catalytic step, Prp16p, another RNA-dependent NTPase, joins the spliceosome, interacts with the 3′ splice site (the junction between intron and exon 2), and drives further rearrangements in the spliceosome (Umen and Guthrie 1995b; Wang and Guthrie 1998). Subsequently, Prp8p, Slu7p, Prp17, Prp22p, and Prp18p are required for completion of the second step (Umen and Guthrie 1995b;

Corresponding author: Jean D. Beggs, Wellcome Trust Centre for Cell Biology, University of Edinburgh, King's Bldgs., Mayfield Rd., Edinburgh EH9 3JR, United Kingdom. E-mail: jbeggs@ed.ac.uk

Schwer and Gross 1998; McPheeters *et al.* 2000). Prp8p and U5 snRNA hold together the ends of the exons that are to be joined (Newman and Norman 1992; Teigelkamp *et al.* 1995; Umen and Guthrie 1995a; Dix *et al.* 1998), whereas Slu7p, Prp18p, and Prp22p are essential *in vitro* for the removal of introns with long branchpoint-3′ splice site distances (Brys and Schwer 1996; Zhang and Schwer 1997; Schwer and Gross 1998). At this stage, U2 snRNA is in close proximity to U5 snRNA and the 3′ splice site (Newman *et al.* 1995; Xu *et al.* 1998). How the catalytic center for the second *trans*-esterification reaction is formed is under debate, but the activity of another U5 snRNP protein, Snu114p, may be needed to locate the 3′splice site (Fabrizio *et al.* 1997; Staley and Guthrie 1998) so that both exons can be precisely aligned by U5 snRNA (O'Keefe and Newman 1998).

After the second splicing reaction, ATP hydrolysis by Prp22p releases the mature mRNA from the spliceosome, the spliceosome dissociates, and the components are recycled. The DEAH-box protein Prp22p is structurally related to the DExH/DEAD-box proteins Prp2p, Prp16p, Prp28p, and Brr2p. RNA unwindase activity has been demonstrated *in vivo* and *in vitro* for Brr2p (Raghunathan and Guthrie 1998; Kim and Rossi 1999) and *in vitro* for Prp16p (Wang *et al.* 1998) and Prp22p (Schwer and Gross 1998; Wagner *et al.* 1998). All these proteins share a central region containing conserved sequence elements implicated in ATP binding and hydrolysis and in RNA binding. Intragenic suppressors of conditional mutations in Prp28p suggest a close proximity between some of these elements (Chang *et al.* 1997). Brr2p contains a second, more C-terminal helicase-like domain with less conserved elements (Lauber *et al.* 1996; Xu *et al.* 1996). This domain tolerates mutations that in the upstream helicase domain confer a dominant negative phenotype (Kim and Rossi 1999), possibly indicating a different function.

To fully understand the interactions that take place within the spliceosome all the components have to be identified and their interactions mapped. Recent purification of subcomplexes and microsequencing of the component proteins increased the number of known yeast splicing factors over those previously identified by genetics and sequence homology (*e.g.*, Gottschalk *et al.* 1999; Stevens and Abelson 1999). Furthermore, six new splicing factors were identified in 16 exhaustive two-hybrid screens (Fromont-Racine *et al.* 1997; Dix *et al.* 1999). Although two-hybrid screens might not reveal all possible functional interactors (Vidal and Legrain 1999), they provide information about putative interacting domains whose function can be analyzed further by other approaches. Furthermore, the sensitivity of this technique allows detection of short-lived interactions that can be expected within the dynamic context of a rearranging spliceosome. We therefore undertook exhaustive two-hybrid screening according to Fromont-Racine *et al.* (1997), using their complex yeast genomic library (FRYL). As baits we used the U5 snRNP proteins Prp8p and Brr2p, the second-step factors Prp18p and Slu7p, and Snu66p, a protein found in Brr2p screens. Snu66p was recently identified as a component of the U4/U5.U6 tri-snRNP (Gottschalk *et al.* 1999; Stevens and Abelson 1999) and, as we show below, is essential for splicing *in vivo* at low temperatures. We observe that Brr2p specifically interacts with Prp2p, Prp8p, Prp16p, Snp1p, Slu7p, and Snu66p. The two-hybrid interactions between Prp16p, Prp8p, Snu66p, Snp1p, and Brr2p were confirmed by co-immunoprecipitation *in vitro* and we conclude that Prp16p recruitment to the spliceosome (Wang and Guthrie 1998) is mediated by Brr2p. We present *in vivo* evidence for the hypothesis that the *prp8-1* allele causes a splicing defect by disrupting the interaction with Brr2p, an interaction that in human cells was found to be independent of U5 snRNA (Achsel *et al.* 1998). The broad range of Brr2p interactions confirms its central role in spliceosomes and suggests a particular function for the C-terminal half, including the second helicase-like domain. This brings forward the hypothesis that, apart from U4/U6 duplex unwinding, Brr2p catalyzes other RNA rearrangements, acting in a synergistic manner with other spliceosomal proteins, including the structurally related proteins Prp2p and Prp16p. Such a cooperation of unwindases, although not previously reported to occur in pre-mRNA splicing, is a common feature of helicases that are part of viral, bacterial, or eukaryotic DNA replication machines. Overall, our combination of exhaustive, iterative two-hybrid screening with functional analyses provides novel information concerning the dynamic control of the order of events in spliceosomes.

MATERIALS AND METHODS

General procedures: Preparation of splicing extracts, immunoprecipitation of proteins and snRNAs, Western detection, isolation of RNA, and hybridization of Northern blots with snRNA probes were as described previously (Teigelkamp *et al.* 1995; Dix *et al.* 1999; Mayes *et al.* 1999). Antibodies were from Santa Cruz Biotechnology, Santa Cruz, California [polyclonal rabbit anti-haemagglutinin (anti-HA); polyclonal rabbit anti-cMYC], Boehringer Mannheim (Indianapolis; 3F10 anti-HA), kind gifts of J. Lewis and D. Xu (12CA5 monoclonal mouse anti-HA), or described previously (anti-Prp8.6 in Teigelkamp *et al.* 1995). For identification of yeast DNA sequences by BLAST search or design of primers the Saccharomyces Genomic Database (http://genome-www.stanford.edu/Saccharomyces/) was used. Homologous proteins were aligned using algorithms Clustal W, Pima, or Mapmaker.

Oligonucleotides sequences are 5′ to 3′: 5′ ACT-PCR (CGCGTTTGGAATCACTACAGGGATG), 3′ ACT-PCR (GAA ATTGAGATATGGTGCACGATGCAC), TNT-ACT (AAACTC GAGTAATACGACTCACTATAGGGAGCCACCATGGCTAG CTTGGGTGGTC).

Two-hybrid screens and direct analysis of two-hybrid interactions: The two-hybrid bait vectors were pASΔΔ (Gal4 DNA-binding domain), pBTM116 (LexA DNA-binding domain),

or their derivatives with +1 or −1 frameshifts in the multiple cloning site. Prey constructs were made in pACTII-stop (Gal4 activation domain; Fromont-Racine *et al.* 1997) or in a +1 derivative. The open reading frames (ORFs) for Slu7p, Prp18p, Prp16p, Prp22p, and Prp2p were cloned directly. The Snu66p baits were made by recombination of prey Su2 and Su5 (Table 1). Full-length *PRP8* and *BRR2* baits and prey, as well as *slt22-1* and *prp16-1* baits, were constructed by gap repair in yeast JDY4, a Sc266c derivative (*MAT***a**, *ade2-101; his*3Δ*200, leu2*Δ*1, trp1*Δ*94, ura3*Δ*99, cir*Δ; a kind gift of J. D. Brown). Linearized plasmids containing both the N and C terminus of each open reading frame were cotransformed with DNA fragments bridging the gap. Successful gap repair of *prp16-1* bait plasmid was scored by the growth defect at 16° for *PRP16/prp16-1* strains. Full-length bait and prey fusions of Prp8p complemented *prp8*Δ strains. Stable expression of prey peptides was verified by Western blotting using 12CA5 anti-HA antibodies. Two-hybrid screens were done by mating (Fromont-Racine *et al.* 1997) or by sequential transformation (Parchaliuk *et al.* 1999) using the FRYL genomic library (Fromont-Racine *et al.* 1997). Direct two-hybrid analyses were done with either mated diploids (in the Gal4-system; Mayes *et al.* 1999) or cotransformed haploid cells (in the LexA-system), which were tested by β-galactosidase assays and on media selecting for expression of the *HIS3* reporter gene. The plates contained different concentrations of the *HIS3* inhibitor triaminotriazole to evaluate the strength of two-hybrid interactions.

Isolation and *in vivo* analysis of cPrp8p mutations that affect two-hybrid interaction with Brr2p: A pool of PCR fragments, generated under mutagenic conditions with primers 5′ACT-PCR and 3′ACT-PCR on prey plasmid E3 DNA (Figure 3A), was repaired into gapped pACTII-stop in yeast L40 cells expressing the LexABrr2p bait. After 1-hr recovery in dropout medium free of tryptophan and leucine, the transformation mixture was plated on histidine-free medium and incubated at 25°. Dot-sized colonies were replica plated onto histidine-free medium with different triaminotriazole (3AT) concentrations (incubated at 30°) or without 3AT (and incubated at 16°, 25°, 30°, and 36°). Comparison of plates yielded candidates for temperature-sensitive, 3AT-sensitive, or 3AT-resistant Brr2p interactions. Rescued prey plasmids were verified to cause the growth phenotype and their c*PRP8* inserts were sequenced. Fragments with mutations responsible for the phenotype were identified after recloning into gapped E3-plasmid. Two mutations, *prp8-28* (clone *E3-N*) and *prp8-52* (clone *E3-H*), showed the strongest temperature sensitivity and 3AT resistance, respectively. These mutations as well as allele *prp8-1* were introduced into *PRP8* on either pRS315 (ARS/CEN, *LEU2*, a gift from D. Xu) or pJU225 (2μ; *TRP1*; Umen and Guthrie 1996). The alleles were tested for their ability to replace the pRS316 (ARS/CEN, *URA3*)/PRP8 maintenance plasmid from strains YDX216 and YDX2258, derivatives of yeast W303 (*ade2-1*, *his3-11*, *leu2-3*, *-112*, *trp1-1*, *ura3-1*, *can1-100*), with a disrupted *PRP8* locus (*prp8*Δ*::HIS3*; kindly provided by D. Xu). YDX2258 differs from YDX216 in mating type (*MAT*α) and the *slt22-1* allele (Xu *et al.* 1996). The *prp8-1*, *-28*, and *-52* plasmids were also tested in yeast YJU75 with a *prp8*Δ*::LYS2* disruption (Umen and Guthrie 1996). The maintenance plasmid was lost by streaking transformants on solid 5-fluoroorotic acid media, also selective for the genomic *PRP8* gene disruption as well as the vector with the tested *prp8* allele. Yeast colonies that grew at 25–30° were restreaked on uracil-containing medium and incubated at different temperatures.

Epitope tagging of genes: Three different haploid strains were made with *BRR2* placed under control of the conditional *MET3* promoter that stimulates strong gene expression but is tightly repressed by methionine (Mountain *et al.* 1991). By targeted integration of an *HIS3*-P_{MET3}-$cMYC_3$ cassette (with flanking sequences homologous to the 5′ untranslated region and the extreme N terminus of *BRR2*) into JDY5 (as JDY4, see above, but *MAT*α), a strain that produced $cMYC_3$-tagged Brr2p was obtained. The second strain, a JDY4 derivative, had a P_{MET3}-controlled, HA_2-tagged *BRR2* gene separated from a truncated *BRR2* gene (with the native promoter) by pUC18 DNA and the *TRP1* gene (see Figure 2B). In the third strain Brr2p was placed under P_{MET3} control without a tag. In an analogous way JDY4 derivatives were obtained in which *SNU66*, *YMR102C*, or *ECM5* were N-terminally tagged with a double HA-epitope.

Immunofluorescence: Yeast cells grown to OD_{600} = 0.5 were fixed with 1/10 volume 37% formaldehyde for 15–30 min, collected, washed with 0.1 M KPO4, pH 7.5/0.7 M sorbitol, and resuspended in 1 ml 250 μg/ml zymolyase 20.000 for 20 min at 30° to digest the cell walls. Cells were collected and resuspended in PBS/0.7 M sorbitol. Fixed cells were immobilized on microscope slides, blocked with 4% milk/0.1% Tween/PBS, and stained overnight at 4° with 3F10 anti-HA antibodies (diluted 1:200) in a humid chamber. After three washes with PBS, cells were incubated with FITC-conjugated Alexa 488 secondary antibody (Molecular Probes, Eugene, OR) for 1 hr at 20° in the dark and examined on an Axioplan2 (Zeiss) microscope attached with CCD camera (Hamamatsu, Bridgewater, NJ).

Gene disruptions and growth analysis: In yeast strain JDY6 (diploid of JDY4 and JDY5, see above) open reading frames *YMR102C*, *YOR308C*, *YNL099C*, and *YPL064C* were entirely substituted by the *HIS3* gene. Correct integration was verified by PCR analysis. Dissected tetrads from diploids with disrupted genes were analyzed at 14°, 16°, 25°, 30°, 36°, and 37° on plates with rich medium (YPDA) or complete synthetic medium lacking histidine and testing glucose, galactose, or lactate as sole carbon source. Growth of *SNU66* and *snu66*Δ*::HIS3* haploids (derived from the same tetrad) was monitored over time in liquid cultures. Cells collected from a preculture incubated overnight at 24° were divided in two, diluted with precooled or prewarmed liquid medium, and further incubated at either 16° or 30°. At particular time points samples of 50 OD units of cells were taken and stored at −80° before RNA was isolated from the cell pellets. Synthetic lethality between *snu66*Δ*::HIS3* and *slt22-1* was tested using the strain YDX22100 (*MAT*α, *ade2-1, his3-11, leu2-3,-112, trp1-1, ura3-1, can1-100, slt22.1*, kindly provided by D. Xu) that was mated to haploid *snu66*Δ*::HIS3*. Dissected spores were allowed to germinate at 25–30° prior to testing for temperature sensitivity at 36° and cold sensitivity at 14°.

Analysis of splicing efficiency by means of an *in vivo* reporter assay: Wild-type and gene-disrupted haploid transformants with either reporter plasmid pJC51 (Rain and Legrain 1997) or pLACZ (Dix *et al.* 1999) were grown in triplicate to mid-log phase (OD_{600} between 0.5 and 1) in noninducing liquid medium at 20° or 30°. Two cultures were then induced with galactose and one was repressed with glucose before incubation was continued for 3 hr (at 20°) or for ½ hr (at 30°). β-Galactosidase activity in each culture was assayed in triplicate according to Rain and Legrain (1997).

Immunoprecipitation of *in vitro*-synthesized peptides: ^{35}S-labeled peptides were produced *in vitro* using Promega's (Madison, WI) TnT-system and [^{35}S]methionine (Amersham, Buckinghamshire, UK) with transcription template PCR products amplified from two-hybrid prey plasmids using primers 3′ACT-PCR and TNT-ACT. Aliquots of $cMYC_3$-tagged *BRR2* splicing extract were depleted of ATP (and thus splicing activity) by endogenous hexokinase at 24° for 20 min after adding glucose and mixed with ^{35}S-labeled fragments and polyclonal anti-

TABLE 1

Details of prey fragments isolated in two-hybrid screens and of other constructs used in this work

Source	Clone		No. of isolates	aa	Remarks
Prp8p					
	Wild type	Construct		1–2413 (end)	(Diagrams in Figure 3A)
	E1	Construct		1649–end	
	E2	Construct		1909–end	
	E3Δ	Construct		2010–2382	
	E3-D	Construct		2010–end	ts with Brr2p, mutation: $G_{2347}D$ allele *prp8-1*
	E3-H	PCR		2010–end	Not ts with slt22.1p; $Y_{2037}H$ & $I_{2051}T$ *prp8-52*
	E3-N	PCR		2010–end	ts with Brr2p, mutation: $I_{2259}N$ allele *prp8-28*
	E3	Prey with Brr2p	1×	2010–end	ts with slt22.1p
	E4	Prey with Brr2p	1×	2033–end	Out of frame: −1
	E5	Prey with Brr2p	1×	2067–end	Out of frame: +1
Prp16p					
	St1	Prey with Brr2p	8×	20–300	(Diagrams in Figure 5A)
	St2	Prey with Brr2p	25×	65–154	
	St3	Prey with Brr2p	3×	87–236	
	St4	Prey with Brr2p	(1×)	109–195	Fished by Brr2ΔM, not in Brr2p screens
	St5	Prey with Brr2p	2×	516–1071 (end)	
	St6	Prey with Brr2p	2×	656–end	
	St7	Prey with Brr2p	1×	896–end	
	St8	Prey with Brr2p	1×	903–end	
	St9	Prey with Brr2p	1×	926–end	
	St10	Prey with Brr2p	1×	940–end	
	wt	Construct		1–end	
	St1Δ	Construct		20–68	
	St5Δ	Construct		516–1033	
	16ΔM	Construct		Δ[141–498]	Bait construct only
Snp1p	Sp1	Prey with Brr2p	7×	−26–299	
	Sp2	Prey with Brr2p	1×	25–300 (end)	
Yp1064p					
	Y1	Prey with Brr2p	1×	61–300 (end)	
	Y2	Prey with Brr2p	1×	72–end	
	Y3	Prey with Brr2p	2×	77–227	
	Y4	Prey with Brr2p	2×	102–end	
	Y5	Prey with Brr2p	2×	125–end	Out of frame: −1
	Y6	Prey with Brr2p	2×	139–240	
Snu66p					
	Su1	Prey with Brr2p	1×	−19–416	Out of frame: −1
	Su2	Prey with Brr2p	4×	8–458	
	Su3	Prey with Brr2p	1×	21–303	Out of frame: −1
	Su4	Prey with Brr2p	6×	99–>458	Fused, not directly, to *YDR278C*-fragment
	Su5	Prey with Brr2p	2×	125–587 (end)	
	Su6	Prey with Brr2p	2×	160–488	Out of frame: +1
	Su7	Prey with Brr2p	3×	161–end	
	Su8	Prey with Brr2p	1×	213–356	
	Su9	Prey with Brr2p	15×	267–447	Fused directly to aa 173-422 of *YDL150W*
	Su10	Prey with Brr2p	1×	272–495	
Brr2p					
	wt	Construct		1–2168 (end)	(Diagrams in Figure 5A)
	ΔM	Construct		Δ[357–1183]	
	ΔNΔM	Construct		112–356 & 1184 end	
	ΔMΔC	Construct		1–356 & 1184 194-1	
	ΔN	Construct		112–end	
	ΔC	Construct		1–1941	
	C	Construct		1729–end	
	B123	Construct		1626–1749	

(*continued*)

TABLE 1

(Continued)

Source	Clone		No. of isolates	aa	Remarks
	B1	Prey	7×	1282–1749	Fished by nPrp8p(2×); Slu7p(4×) and Snu66p(1×)
	B2		2×	1497–1760	Fished by Fab1p
	B3		1×	1626–end	Fished by Snu66p and fused to *YER026-27C* intergenic fragment
Prp18p					
	Et1	Prey with Slu7p		39–251 (end)	
	Et2			101–end	
Prp22p					
	Tt1	Prey with Slu7p		142–747	(Diagrams in Figure 5A)
	Tt2			471–806	
Prp6p	S1	Prey		131–733	Fished by Snu66p
Prp39p	Tn1	Prey		5–437	Fished by Prp8p

Like Fromont-Racine *et al.* (1997) we obtained out-of-frame prey fusions (indicated by underlining) for which readthrough fusion products were detected on Western blots (data not shown). Furthermore, an out-of-frame fusion of a Snu66p fragment (clone Su6) was functional in a complementation assay. The Snu66p residues (aa 272-447) that are required for strong Brr2p interaction (resistant to 10–20 mM 3AT; data not shown) or essential (but not necessarily sufficient) for full complementation of *snu66*Δ at 14° (aa 448–458; data not shown), lie in between the N- and C-terminal regions most highly conserved between Snu66p homologs from yeast (YOR308C), human (NCBI protein accession no. BAA24056.1), worm (NCBI protein accession no. AAB52287.1), or fission yeast (GenBank accession no. SPAC167.03C).

cMYC antibodies in conditions of 150 mM NaCl. After a half-hour incubation on ice protein, A-Sepharose (Sigma, St. Louis) was added and the mixtures were rotated at 4° for 2 hr. The beads were washed three times with IP buffer containing 150 mM NaCl, after which the attached proteins were eluted with loading buffer at 60°. Eluted proteins and supernates (50%) were separated on 10% SDS polyacrylamide and visualized by fluorography on Kodak Biomax MR film after fixing the gel in 10% glacial acetic acid/30% methanol.

RESULTS

Two-hybrid screens: The characteristics of our exhaustive two-hybrid screens and of the proteins found as prey are presented in Figure 1 (classified according to A1, A2/A3, A4, and B prey categories; Fromont-Racine *et al.* 1997). The parameters of functionally interesting prey fusions are listed in Table 1. The discussion focuses predominantly on interactions between splicing factors and the validation of these interactions by other approaches; however, the A1, A2, and A3 category prey are considered to be potentially interesting and the analysis of these continues.

We started with Prp18p and Slu7p as bait fusions. The Prp18p screen was highly selective, the main prey (of the A1 category) being Slu7p. Ten different Slu7p fragments (54 clones in total) share a region of overlap (residues 170–249) that was sufficient for the interaction (M. Albers, R. W. van Nues and J. D. Beggs, unpublished results; also implicated by data reported by Zhang and Schwer 1997). As bait, Slu7p fished the C-terminal regions of Prp18p (clone Et2) and Brr2p (clone B1), as well as the DEAH-box region of Prp22p (see Table 1 for details). As Prp18p and Slu7p are known to interact genetically (see references in Umen and Guthrie 1995b) and physically (Zhang and Schwer 1997), the specificity of these screens gave us a high level of confidence in the quality of the genomic library and the effectiveness of the technique (Fromont-Racine *et al.* 1997).

Screens with the full-length U5 snRNP protein Brr2p were also highly informative. Brr2p retrieved the C terminus of another U5 snRNP protein, Prp8p, in three different fusions (prey E3, E4*, and E5*), both termini of Prp16p (St1–3 and St5–10), the middle of Snu66p (Su1–Su10), and almost complete Snp1p (Sp1 and Sp2; see Table 1 for details of all these prey fusions). Furthermore, there are some statistically significant interactions of Brr2p with proteins not directly implicated in splicing, such as the finding of a cyclophilin of unusual length, Ypl064p (Table 1). Mammalian cyclophilins have been described that co-localize with splicing factors (Mortillaro and Berezney 1998) and tri-snRNPs (discussed in Gottschalk *et al.* 1999; Stevens and Abelson 1999) but no yeast cyclophilins were reported to be stably associated with the yeast U4/U6.U5 tri-snRNP (Gottschalk *et al.* 1999; Stevens and Abelson 1999). Similarly, Brr2p interacted with WD40 fragments of the uncharacterized Ymr102p, which might conceivably be the yeast orthologue of the 40-kD human U5 snRNP protein (Achsel *et al.* 1998), although this was not found in purified yeast tri-snRNPs (Gottschalk *et al.* 1999; Stevens and Abelson 1999). Selection of the N terminus of Fab1p as prey of Brr2p remains to be evaluated

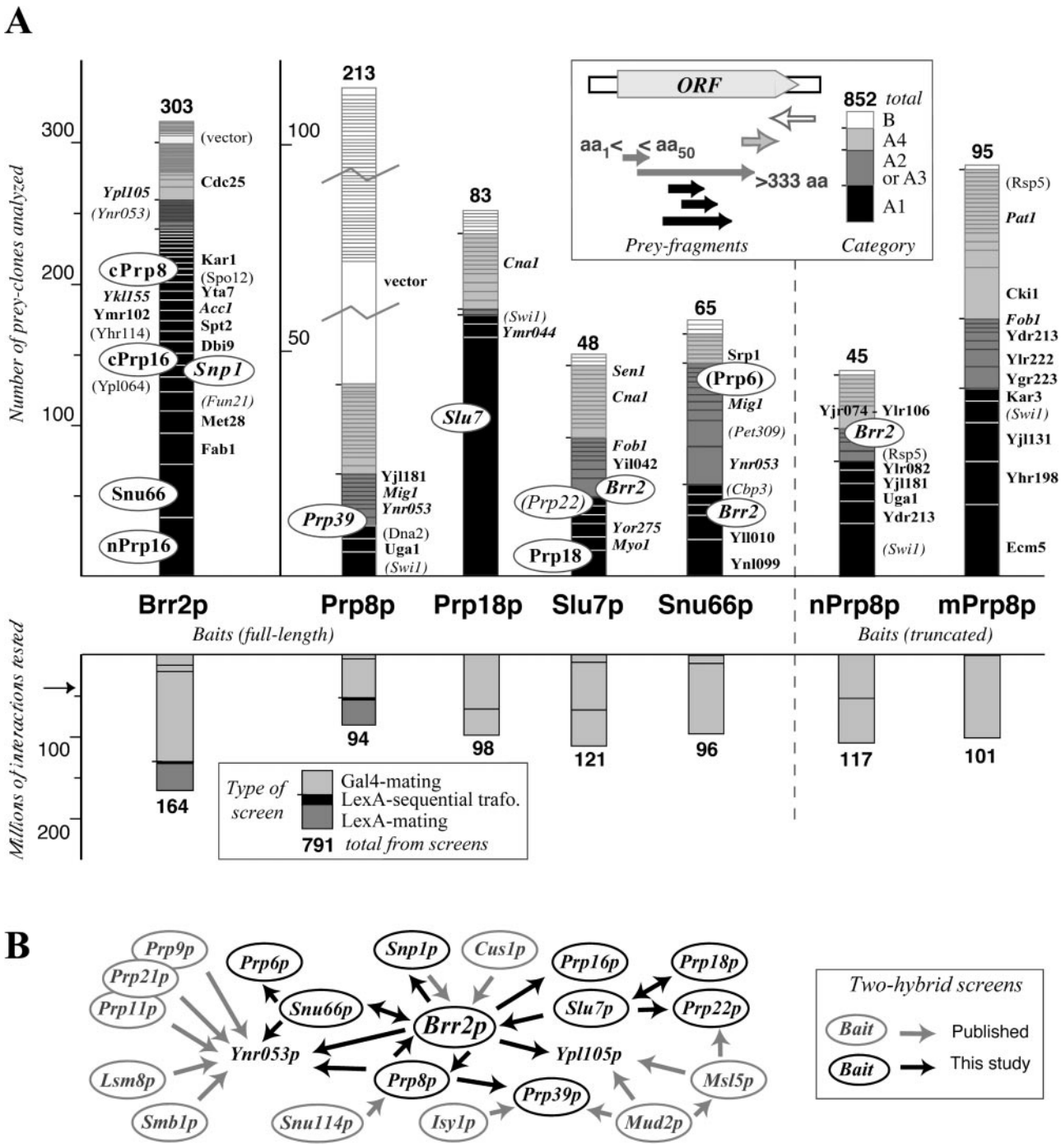

FIGURE 1.—(A) Results of two-hybrid screens with full-length or truncated U5 snRNP-associated splicing proteins as bait. (Top) Distribution profiles of prey proteins, which are classified according to A1, A2/A3, A4, and B categories (FROMONT-RACINE *et al.* 1997) and partitioned with respect to the number of clones from the same genomic locus. Multiple fragments overlapping a protein interaction domain constitute prey of category A1 and indicate a significant two-hybrid interaction. Interaction domains that start within 50 amino acids of the N terminus of the protein (category A2) or that require >333 amino acids to be present in the prey fusion (category A3) will be underrepresented and therefore are statistically relevant even if found only as a single clone. Other coding prey fusions fall within category A4, whereas category B consists of noncoding intergenic, or antisense, fusions or of prey derived from mitochondrial or ribosomal DNA (see inset). Known splicing factors (in ovals), previously described loci (in italics; FROMONT-RACINE *et al.* 1997; DIX *et al.* 1999), or open reading frames with statistically significant occurrence are printed alongside each column. Weakly interacting prey fusions are within parentheses. Total number of prey clones analyzed is indicated above each column. Note the threefold larger scale for the Brr2p column. Zigzags in the Prp8p-B class signify that 40% of cut segments are shown. (Bottom) Characteristics of the two-hybrid screens. Total number of potential interactions tested with each bait (*i.e.*, cells with both bait and prey plasmid) is shown under the columns, which are divided according to the different experiments done (see inset and MATERIALS AND METHODS). The arrow indicates the practical threshold of 45 million potential interactions tested to reach exhaustive coverage of the FRYL yeast genomic library (FROMONT-RACINE *et al.* 1997, 2000). (B) Overlap with previously described two-hybrid screens using splicing factors as bait (FROMONT-RACINE *et al.* 1997; DIX *et al.* 1998, 1999).

but, provocatively, a Brr2p fragment was retrieved in a Fab1p screen (R. H. Michell, R. W. van Nues, J. D. Beggs and S. K. Dove, unpublished results; Table1), and the finding that PIP5-kinases like Fab1p are not only vacuolar but also co-localize with splicing factors in nuclear speckles (Boronenkov *et al.* 1998) suggests this may be a functional protein interaction. In a partial screen with a truncated Brr2p lacking the first helicase domain (clone Brr2ΔM; Table 1), the most abundant A1 prey were Dbi9p, Fab1p, and Pet127 (data not shown), while Prp16p was found once (clone St4; Table 1).

Full-length Prp8p as bait did not produce such obviously specific interactions (although the bait fusion protein proved to be functional by complementation of *prp8*Δ strains; data not shown). The only known splicing factor to be found as prey was the U1 snRNP protein Prp39p, of which one A2/A3 clone with the N-terminal tetratricopeptide repeat (TPR) region was found twice. As Prp8p is very large (280 kD), we also performed screens with several Prp8p fragments that have been successfully used to raise antibodies (Jackson *et al.* 1988) or that have been implicated in regulation of 3′ splice site fidelity ("mPrp8p," amino acids 1649–2115; Figure 3A; Umen and Guthrie 1995a). These had mixed success as baits. The N-terminal region of Prp8p, encompassing proline-rich repeats and a basic segment ("nPrp8p," residues 1–263; Figure 3A), fished a C-terminal fragment of Brr2p (clone B1, Table 1). The nPrp8 region also turned out to form the main contact with the fragment of Prp39p isolated in the full-length Prp8p screen (data not shown). This seems to be a specific interaction, as nPrp8p did not associate with the TPR-containing Prp6p fragment found by Snu66p, and the Prp39p prey did not interact with Snu66p (data not shown). Intriguingly, in every screen with a Prp8p fragment as bait we retrieved fragments with the middle region of the uncharacterized protein Ydr213p. Kuhn and Brow (2000) also performed two-hybrid screens with fragments of Prp8p, one of which corresponded to an N-terminal region. None of the prey identified in our screens with Prp8p baits coincided with theirs, but they did not find two-hybrid interactions with any known splicing factors.

A screen with Snu66p, isolated as one of the main prey with Brr2p, yielded the C terminus of Brr2p (clones B1 and B3; Table 1), a large fragment of Prp6p with TPR repeats (clone S1), as well as Ynl099p and Yll010p. Ynl099p is a nonessential protein (our data, see below, and Saiz *et al.* 1999) with a phosphatase-like domain, present in the prey fragments, that is supposed to interact with phosphoserine, -threonine, or -tyrosine residues (Wishart and Dixon 1998). Ynr053p was found as an A2/A3 category prey in screens with Snu66p, Brr2p, and Prp8p and has been found by others in screens with five other splicing factors (Prp9p, Prp11p, Prp21p, Smb1p, and Lsm8p; Fromont-Racine *et al.* 1997). Ynr053p is similar to a human breast tumor-associated auto-antigen. Interestingly, the human homologue of *SNU66*, *hSART1* (NCBI protein accession no. BAA24056.1), has also been isolated as a tumor antigen (Kikuchi *et al.* 1999), whereas the Snu66p-interacting fragments of Yll010p show high homology with human proteins hY22 and hOS4, the genes of which are deleted or amplified in carcinoma cell lines (Ishikawa *et al.* 1997; Su *et al.* 1997).

In all these experiments we screened the complete FRYL yeast genomic library (Fromont-Racine *et al.* 1997; see Figure 1). Prp8p and Brr2p screens with different two-hybrid systems (Gal4 *vs.* LexA) or different methods (mating the yeast strains that carry bait or prey plasmids *vs.* sequential transformation of the library and bait plasmids) yielded comparable results that were characteristic for each bait protein. Figure 1B presents a schematic overview of interactions detected between known splicing factors. This highlights the central position of Brr2p as both bait and prey in the network of interactions and shows the overlap with results of two-hybrid screens described previously (Fromont-Racine *et al.* 1997; Dix *et al.* 1998, 1999).

In subsequent experiments we sought evidence for the functional significance of these two-hybrid interactions through genetic analyses, localization studies, and co-immunoprecipitation experiments.

Genetic analysis of uncharacterized open reading frames: We further analyzed five open reading frames that were uncharacterized at the time. *YOR308C* (*SNU66*), *YMR102C*, and *ECM5* were epitope tagged by adding a double HA epitope to the N termini (materials and methods) and the *YOR308C*, *YPL064C*, *YMR102C*, and *YNL099C* ORFs were disrupted by replacing the entire open reading frame with *HIS3* (materials and methods). Growth and localization studies allowed elucidation of gene function only in the case of *YOR308C* (*SNU66*; the second most abundant open reading frame found in our Brr2p screens). None of the other disrupted genes was essential for growth under the various conditions tested (materials and methods). However, although haploid *snu66*Δ*::HIS3* cells showed no apparent growth defect at 30°, they did not grow at 14° (Figure 2A) and grew only very slowly at 16°. The growth defect at 14° was specific for the disruption of *SNU66* as demonstrated by complementation of the defect by full-length Snu66p or some of the Snu66 fragments fished in Brr2p screens (data not shown). Deletion of *SNU66* is not synthetic lethal with the *BRR2* allele *slt22-1*.

Nuclear localization of Brr2p and Snu66p: To evaluate the role of *YOR308C* we tested the cellular localization of the gene product using strains in which the *BRR2* or *SNU66* gene was N terminally tagged with a double HA epitope (Figure 2B). By addition of methionine to the medium the *MET3* promoter that controlled expression of tagged *SNU66* (P_{MET3}*:HA*$_2$*:SNU66*) was effectively repressed as observed by the strong decrease of HA-specific Western signals, although cell growth was not

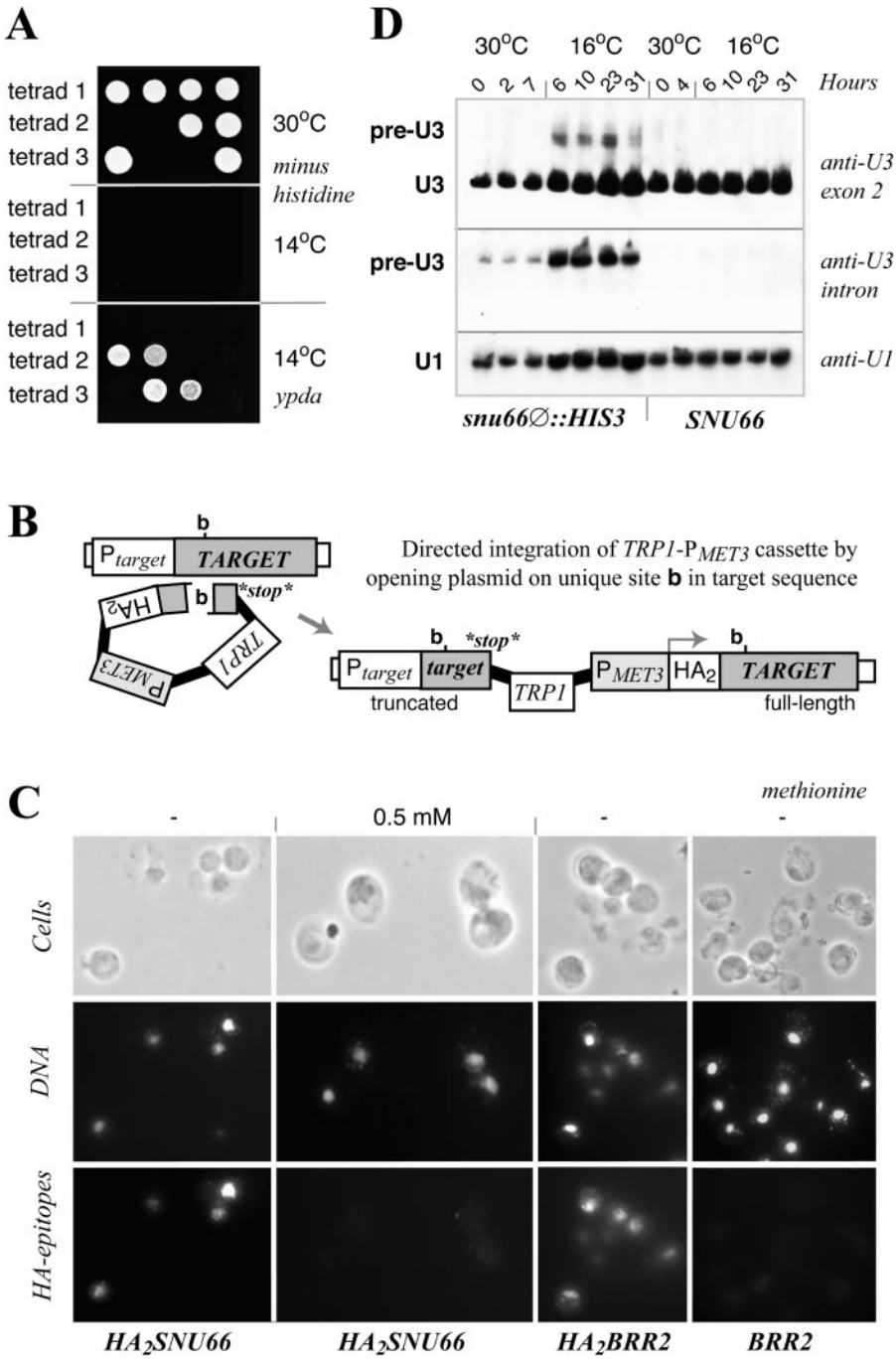

FIGURE 2.—Snu66p localizes to the nucleus, whereas disruption of *SNU66* causes a cold-sensitive growth and splicing phenotype. (A) Tetrad dissection of sporulated *snu66*Δ*::HIS3/ snu66*Δ*::HIS3* (tetrad 1) or *SNU66/snu66*Δ*::HIS3* (tetrads 2 and 3) diploid cells. Haploid *snu66*Δ cells are not viable at 14° and at 16° have twice the doubling time of wild-type cells (data not shown). (B) The chromosomal *SNU66* and *BRR2* genes were put under control of the conditional *MET3* promoter by insertion of a *TRP1*-P_{MET3} cassette that, in the case of N-terminally tagged proteins, also included a double haemagglutinin (HA_2) sequence. (C) As shown by indirect immunofluorescence, tagged Brr2p and tagged Snu66p display nuclear localization, as for DNA stained with DAPI. Cells containing untagged protein or with the *MET3* promoter repressed by addition of 0.5 mM methionine to the growth medium did not stain with anti-HA antibodies. (D) Northern analysis of total RNA isolated from wild-type or *snu66*Δ cultures incubated at 30° or 16°. Samples were taken at the indicated time points after the temperature shift from 24° (see MATERIALS AND METHODS). Pre-U3 snoRNA accumulated in the *snu66*Δ strain at 16° and was even detectable at 30°. In contrast, the levels of U1 snRNA (as well as U2, U4, U5, and U6, not shown) did not increase at 30°, although at 16° some accumulation was observed.

affected (see also Figure 2C). Under these conditions P_{MET3}*:HA*$_2$*:BRR2* cells stopped growing, since *BRR2* is an essential gene (LAUBER *et al.* 1996; LIN and ROSSI 1996; NOBLE and GUTHRIE 1996; XU *et al.* 1996).

By indirect immunofluorescence we found that, as expected for a pre-mRNA splicing factor, tagged Brr2p localized in the nucleus (Figure 2C): the 4′6-diamidino-2-phenylindole (DAPI) staining of DNA merged with the immunostaining obtained with anti-HA primary antibodies. HA_2-Snu66p displayed clear nuclear accumulation in a protein-specific manner, as upon repression of the *MET3* promoter only background signals were observed (Figure 2C). The localization of Snu66p was analyzed more precisely by immunoprecipitation experiments with anti-Prp8p and anti-HA antibodies. HA_2-Snu66p was present in Prp8p-containing complexes and Northern analysis of RNAs isolated from anti-HA antibody precipitates showed that U5, U4, and U6 snRNAs associated specifically with tagged Snu66p under non-splicing conditions, whereas U1 and U2 snRNAs and U3 snoRNA did not (data not shown, but see GOTTSCHALK *et al.* 1999).

Snu66p is a splicing factor required for efficient splicing: Snu66p was previously shown to copurify with U4/

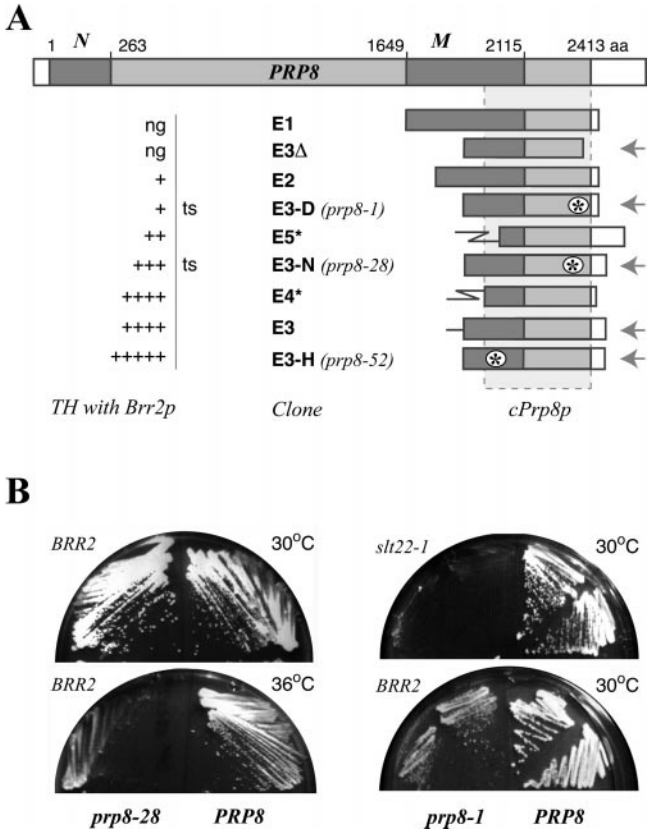

Figure 3.—Analysis of interactions between Brr2p and the C terminus of Prp8p. (A) Prp8p fragments isolated as prey with Brr2p. The *PRP8* coding sequence is shown as a gray bar with darker areas marking the N-terminal and M fragments that were used as bait fusions (Figure 1). Open bars are flanking sequences. Numbers of amino acids (aa) are indicated. Because of either +1 or −1 frameshifts (indicated by zigzags), only low levels of complete fusion peptides E4* and E5* were expressed (as detected by Western analysis). The strength of interaction between Brr2p bait and the Prp8p fragments is indicated in terms of growth on plates containing different levels of triaminotriazole (mM 3AT); *i.e.*, >20 mM (+++++), 20 mM (++++), 10 mM (+++), 5–10 mM [++(+)], 5 mM (++), 2 mM (+), and 0 mM 3AT (±); ng means no growth on medium lacking histidine (in absence of 3AT). Mutants marked with a gray arrow were used in subsequent experiments. In the LexA two-hybrid system full-length Brr2p interacted strongly with the last 400 amino acids of Prp8p. This interaction is reduced progressively upon extension of the interacting segment into regions upstream of residue 2010. Full-length Prp8p did not bind to Brr2p in two-hybrid assays. Furthermore, contrary to wild type (clone E3), the *prp8-1* allele (clone E3-D) or the *prp8-28* (clone E3-N) mutation generated by PCR mutagenesis resulted in a Brr2p interaction that was weakened at 30° and abolished at 37° (temperature sensitive). At 37° wild-type Prp8p fragments but not the E3-H mutant (*prp8-52*) lost the interaction with slt22-1p (mutant Brr2p) in the Gal4 two-hybrid system. (B) *Prp8* mutations were analyzed *in vivo* by a plasmid shuffle experiment. Otherwise isogenic *slt22-1* (mutant *brr2*) or *BRR2* strains with a disrupted *PRP8* genomic locus and wild-type *PRP8* on a *URA3* plasmid were transformed with plasmids carrying *prp8* alleles. Incubation on media with 5-fluoroorotic acid, which permits growth of only *ura*$^-$ (plasmid-free) cells, showed that the *prp8-1* allele caused synthetic lethality in *slt22-1* strains (right). The *prp8-28* mutation was not synthetic lethal with *slt22-1* (data not shown) but it prevented the growth of *BRR2* strains at 36° (left). Furthermore, the PCR-generated *prp8-52* mutation did not show a phenotype *in vivo* nor did it suppress the temperature sensitivity of *slt22-1* strains despite its strengthening of two-hybrid interaction in both Brr2p and slt22-1p baits (data not shown). For all alleles tested the plasmid shuffle was complete, because afterward the strains needed uracil in the medium for growth (data not shown).

U6.U5 tri-snRNPs and spliceosomes (Gottschalk *et al.* 1999; Stevens and Abelson 1999), and an antibody inhibition experiment was presented as evidence for its requirement for splicing *in vitro* (Gottschalk *et al.* 1999); however, as noted by Gottschalk *et al.* (1999), the function of the entire tri-snRNP complex might be inhibited by steric hindrance due to antibody binding. Using two different splicing assays, we obtained conclusive evidence that Snu66p is required for normal splicing *in vivo*. As demonstrated by Northern analysis (Figure 2D), pre-U3 RNA accumulated in *snu66Δ::HIS3* cells at 16° but not in wild-type *SNU66* cells. Even at 30° a mild defect in splicing was observed both by Northern analysis with a probe specific for the U3 intron (Figure 2D) and by primer extension analysis (data not shown). The observation that absence of Snu66p is detrimental at low temperatures suggests a kinetic or assembly defect (Noble and Guthrie 1996).

We observed a comparable cold-sensitive splicing defect when we assessed splicing activity in *snu66Δ::HIS3* cells with a sensitive β-galactosidase assay (Rain and Legrain 1997; Dix *et al.* 1999). This assay is based on two *LACZ* reporter genes, one containing a poorly spliced intron, the other an intronless control. A comparison of the levels of β-galactosidase activity with these reporters is a measure of splicing activity. At 20° β-galactosidase activity in *snu66Δ::HIS3* cells was only 40% of the level in wild-type *SNU66* cells, and at 30° the activity in mutant cells was ~60% of the wild-type level, whereas the level of expression of the intronless reporter was essentially identical in the two strains (data not shown). In similar experiments there was no significant difference in β-galactosidase activity from the two reporters in strains with gene disruptions of *YPL064C*, *YMR102C*, or *YNL099C* (data not shown).

Genetic analysis of the interaction between Brr2p and cPrp8p: Fragments longer than ~700 bp are underrepresented in the FRYL library of prey plasmids (Fromont-Racine *et al.* 1997), which might explain why only three cPrp8p fragments (clones E3, E4*, E5*; Table 1 and Figure 3A) were found in our Brr2p screens, as all were long. Further analysis of this interaction by mutagenesis of cPrp8p fragments showed that this interaction is easily weakened (measured by the level of resistance to 3AT, which inhibits the *HIS3* two-hybrid reporter gene). N-terminal extension (clones E1 and E2) or C-terminal truncation of the cPrp8p prey fragment

(clone E3Δ) greatly reduced the affinity for Brr2p (Figure 3A) but did not affect the stability or expression of the prey peptides as checked by Western analysis (data not shown). This suggests that the Brr2p interaction with cPrp8p is weakened by the presence of Prp8p regions implicated in 3′ splice site recognition (Umen and Guthrie 1996), crosslinking to the 5′ splice site (Reyes *et al.* 1999), U4cs suppression (Kuhn *et al.* 1999), and U2 synthetic lethality (Xu *et al.* 1998; D. Xu, personal communication)—upstream of residue 2010.

We searched by reverse two-hybrid analysis (Vidal and Legrain 1999) for *cPRP8* point mutations that affect interaction with Brr2p in growth assays at different temperatures. The strength of the interaction was measured as the level of resistance to 3AT and was confirmed by measuring the β-galactosidase activities resulting from expression of the *LACZ* reporter gene. As a candidate for such a mutation that might affect the interaction, the *prp8-1* allele was tested directly. Interestingly, Brr2p interaction was severely affected by this mutation at 30° and abolished at 36° (clone E3-D; Figure 3A). A screen for interaction mutants yielded five cPrp8p clones with reduced and temperature-sensitive interaction with Brr2p, two mutants with reduced interaction, and five mutants that interacted more strongly. The *prp8-28* temperature-sensitive mutation that changed the semiconserved isoleucine-2259 to asparagine was located near the *prp8-1* allele ($G_{2347}D$; Hodges *et al.* 1995) but had a less detrimental effect on Brr2p interaction. Comparison of clones E5* and E4* suggests that Prp8p amino acids 2033–2067 are not essential for, but enhance the strength of, two-hybrid interaction with Brr2p. We isolated mutations (*e.g.*, *prp8-52* in clone E3-H) in this region that enhance the affinity for Brr2p. The *prp8-52* allele also suppressed the heat-sensitive growth defect caused by the *slt22-1* mutation (in the first helicase region of Brr2p) at 37°, indicating that the *prp8-52* mutation affects a functionally important interaction with Brr2p. The *prp8-52* allele contains two amino acid changes ($Y_{2037}H$ and $I_{2051}T$) of which the tyrosine to histidine substitution appears to be the most important because it was found in another clone that displayed the same phenotype but also carried a second mutation ($K_{2018}E$).

Full-length *prp8* genes carrying these mutations were constructed for further analysis *in vivo*. *BRR2* and *slt22-1* strains that contain a chromosomal *prp8*Δ plus a plasmid-borne *prp8-1*, *prp8-28*, or *prp8-52* allele were produced by a plasmid-shuffle system (kindly provided by D. Xu; materials and methods). In contrast to the *prp8-52* allele that behaved like wild-type *PRP8*, the *prp8-28* allele did not support growth at elevated temperatures in *BRR2* cells. At 36° these cells grew very slowly (Figure 3B, left) and at 37° they were dead. The *prp8-1* allele had a more severe effect; it caused a mild growth defect in *BRR2* cells at 30°, whereas the *prp8-1, slt22-1* double mutant was not viable at this temperature (Figure 3B, right). The *prp8-28* and *prp8-52* alleles did not cause such synthetic lethality. Thus, mutations of Prp8p that affect its interaction with Brr2p caused growth defects comparable to the reduced affinity for Brr2p.

Co-immunoprecipitation experiments validate two-hybrid interactions of Brr2p with Prp16p, Snp1p, and Snu66p: As an independent means of testing the Brr2p interactions detected in the two-hybrid screens, and to check the stability and strength of these interactions, we did co-immunoprecipitation experiments using *in vitro* ^{35}S-labeled prey peptides and yeast extract containing triple cMYC-tagged Brr2p. We also tested the effects of the *prp8-1*, *prp8-28*, and *prp8-52* mutations. As shown in Figure 4A, the wild-type Prp8 peptide (E3) and the one containing the *prp8-52* mutation (E3-H) precipitated with $cMYC_3$-tagged Brr2p, confirming that Brr2p and Prp8p associate, directly or indirectly. In contrast, none of the mutant peptides E3-D, E3-N, and E3Δ that had displayed reduced two-hybrid interaction with Brr2p was detectably co-immunoprecipitated with Brr2p. These results also demonstrate the specificity of the cMYC antibodies (*e.g.*, that they do not stick to the peptide derived from pACTII sequences that were amplified with each DNA template used for the *in vitro* transcription/translation reaction; see materials and methods). Thus, the two-hybrid interactions accurately indicate the ability of these two splicing factors to associate (directly or indirectly).

Similarly, we observed specific coprecipitation of Snp1p (Sp1), Snu66p (Su2), and nPrp16p (St1, St2), cPrp16p (St10) fragments (Figure 4, B and C) that strongly supports the two-hybrid results. In contrast, the weakly interacting, but frequently found, Ypl064p prey fusions did not coprecipitate with $cMYC_3$-Brr2p under our stringent test conditions (Figure 4B). Interestingly, ~20-fold more of the ^{35}S-labeled cPrp8 protein precipitated with $cMYC_3$-Brr2p (fragment E3; Figure 4A) than did nSnu66p (fragment Su2; Figure 4B; note that both prey peptides contain nine methionines). Also in the two-hybrid assay we found that the interaction of Brr2p with cPrp8p appears to be stronger than with Snu66p. When abundance of prey peptides was a limiting factor for interaction (*e.g.*, in the case of prey fusions requiring a frameshift for complete expression), the interaction of Snu66p (clones Su1* or Su6*; Table 1) with Brr2p was markedly down (*i.e.*, lost after addition of 3AT to the medium) compared to cPrp8p (clones E4* and E5*, resistant to 20 and 5 mm 3AT, respectively; Figure 3A).

Both the N- and C-terminal fragments of Prp16p that interacted with Brr2p correspond to regions of Prp16p that have been reported to bind the spliceosome (Wang and Guthrie 1998). The N-terminal region of Prp16p most frequently found in our Brr2p screens (Table 1 and Figure 1) forms the primary contact during Prp16p recruitment under splicing conditions (Wang and Guthrie 1998). To directly test for interaction between Brr2p and nPrp16p in yeast cell extracts, ATP-depleted

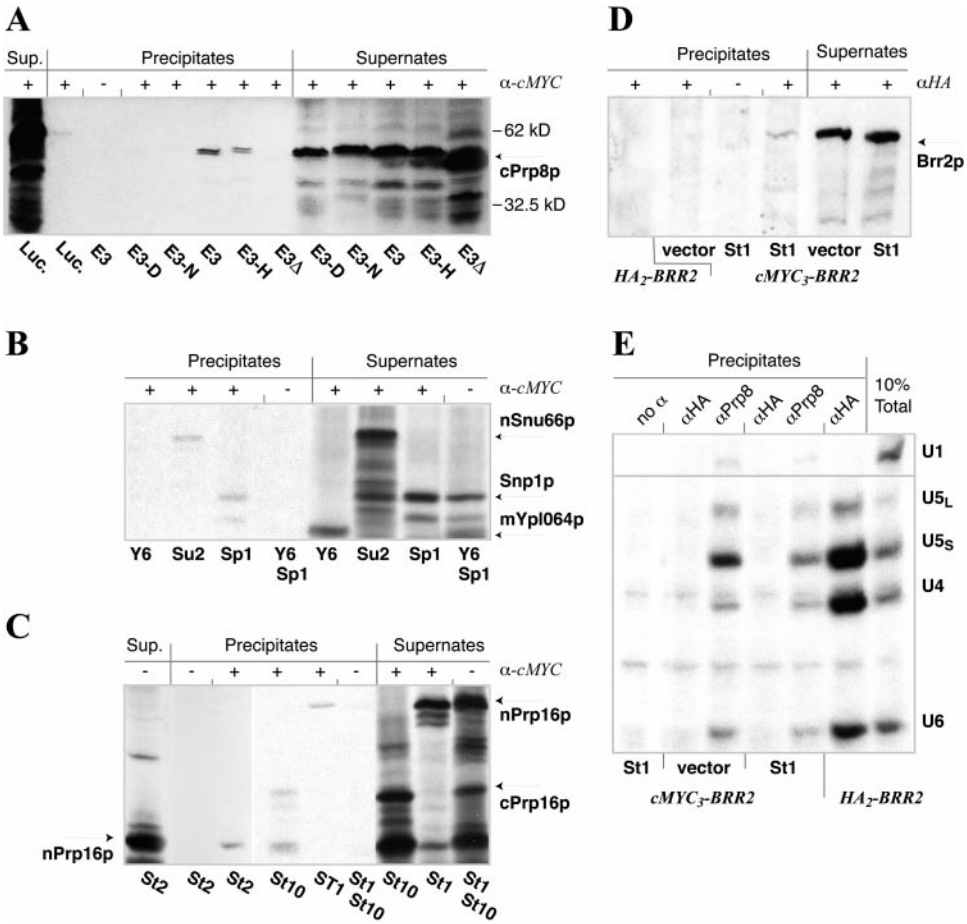

FIGURE 4.—Analysis of interactions between Brr2p and (A) the C-terminal region of Prp8p; (B) Snu66p, Snp1p; and (C) the N- and C-terminal regions of Prp16p by co-immunoprecipitation experiments with yeast extract containing $cMYC_3$-tagged Brr2p and [^{35}S]methionine-labeled peptides produced *in vitro*. Mock precipitations without antibodies were included as a negative control as well as luciferase (Luc. in A). Although Ypl064p-fragments were frequently found in Brr2p screens, their two-hybrid interaction with Brr2p was weak and no co-immunoprecipitation with tagged Brr2p was observed (B). Compared to A, the precipitates in B and C are relatively overexposed. (D) $cMYC_3$-tagged Brr2p co-immunoprecipitated with nPrp16p prey fusions pulled down with anti-HA antibodies. (E) Under these conditions no snRNAs were detected in the anti-HA precipitates.

(to prevent spliceosome formation) extracts from *cMYC$_3$-BRR2* strains carrying an nPrp16 prey plasmid (clone St1) were treated with anti-HA antibodies directed to the internal HA epitope of the nPrp16p fusion peptide. In this setup, tagged Brr2p and the nPrp16p fusion peptide are relatively overproduced so that both could be titrated away from other spliceosomal components in the case of a direct interaction. Western blotting using anti-cMYC antibodies (Figure 4D) demonstrated that $cMYC_3$-tagged Brr2p co-immunoprecipitated specifically with the fusion of the N-terminal Prp16p fragment without detectable association of any spliceosomal snRNAs (Figure 4E). In parallel experiments, full-length Prp16p also co-immunoprecipitated with tagged Brr2p (data not shown).

A network of contacts between splicing proteins: In our screens we observed interactions between Brr2p as bait and splicing factors Prp16p, Snu66p, Prp8p, or Snp1p on one hand and between Slu7p, Snu66p, or nPrp8p as bait with Brr2p on the other (Figure 1). To delineate the Brr2p portion responsible for each interaction, we tested two-hybrid interactions between all these proteins and prey peptides. Brr2p deletion variants, slt22-1p, truncated Prp16p, prp16-1p and other DEAH-box proteins, Prp22p (prey of Slu7p), and Prp2p were also included (see Figure 5A and Table 1 for definition of clones). The results of these direct two-hybrid tests (Figure 5B) not only confirmed the specificity of our two-hybrid screens but also showed two-hybrid interactions of Brr2p with Prp2p and of Prp16p with Prp22p.

Interestingly, a near-exhaustive screen with Prp16p as bait retrieved, as the sole prey, two different Prp22p fragments (with fusions starting at residues 390 and 647; A. COLLEY and J. D. BEGGS, unpublished results), which limits the Prp16p-interacting region to Prp22p residues 647–806. Note that the termini of Prp16p (*e.g.*, St1p or St6p as prey) interact with Brr2p but not with Prp22p, whereas deletion of the internal GKT-DEAH region from Prp16p (bait 16ΔM) reduced the Prp22p interaction but did not affect the contact with Brr2p. Similarly, the *prp16-1* allele ($Y_{386}D$), located within the DEAH-box region, affected the interaction with Brr2p only slightly at 30° (more so at 14°) but made the interaction with Prp22p temperature sensitive (as the interaction of Prp16p with clone Tt2 at 36° was disrupted by *prp16-1*). Thus, the interactions of Prp16p with Brr2p and with Prp22p appear to be independent.

In contrast to Prp16p that interacted through either terminus with Brr2p, *PRP2* clone T1 (the C-terminal half, starting at amino acid 460) did not interact, whereas full-length Prp2p interacted with Brr2p. The failure to retrieve Prp2p in Brr2p screens may therefore

be explained by a lack of sufficiently long inserts in the FRYL yeast genomic library (Fromont-Racine *et al.* 1997).

The C terminus of Brr2p is a protein interaction domain, but is not sufficient for cPrp8p interaction: Deletion analysis of Brr2p showed that the C-terminal Brr2p

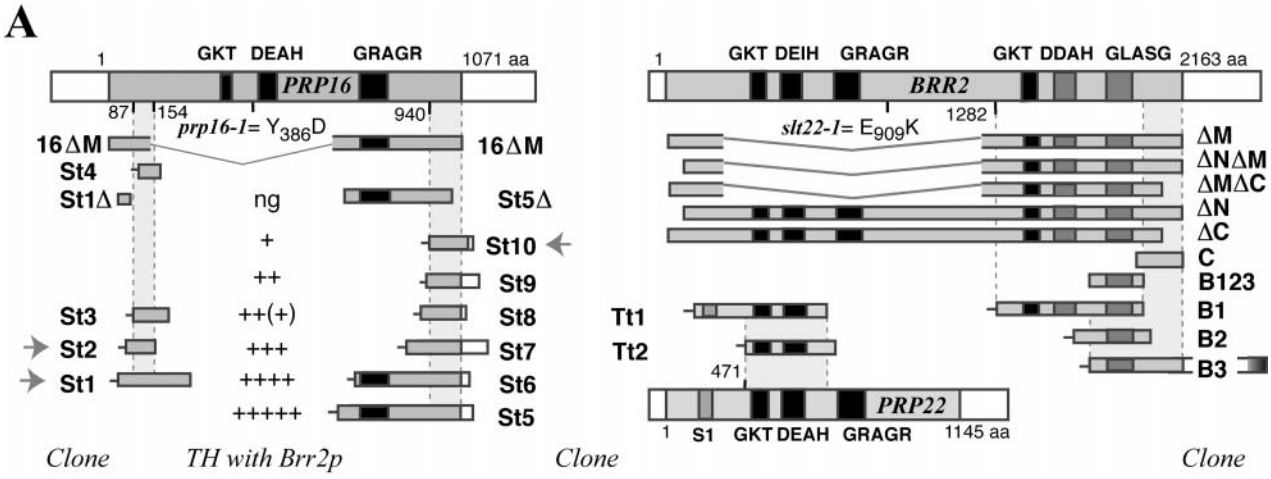

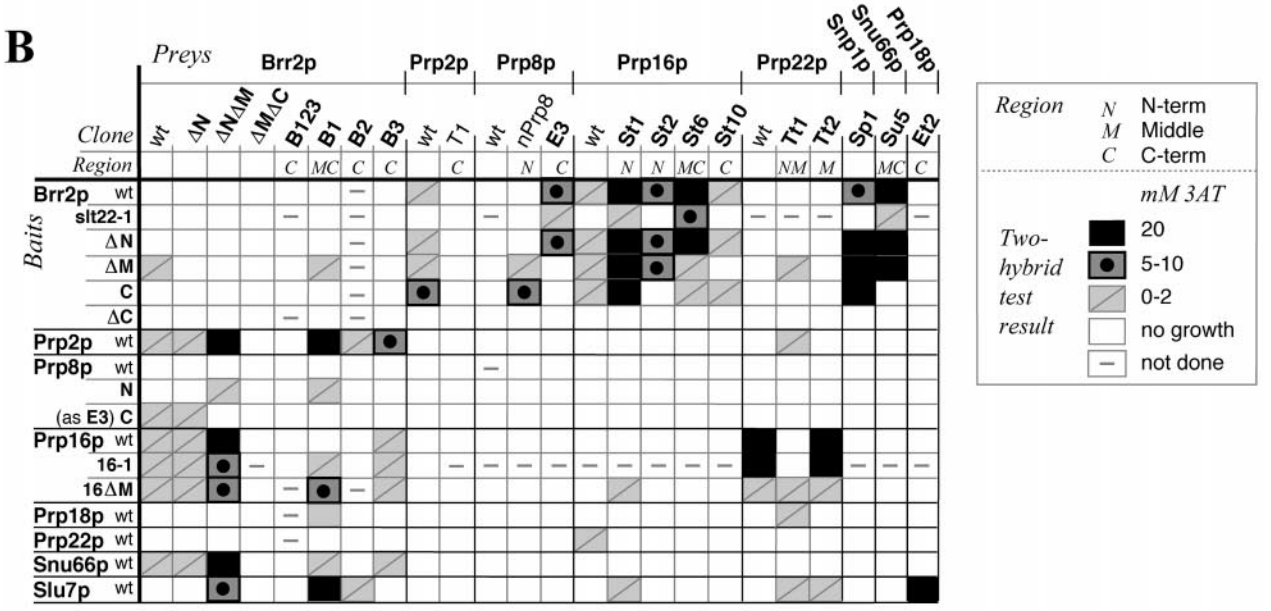

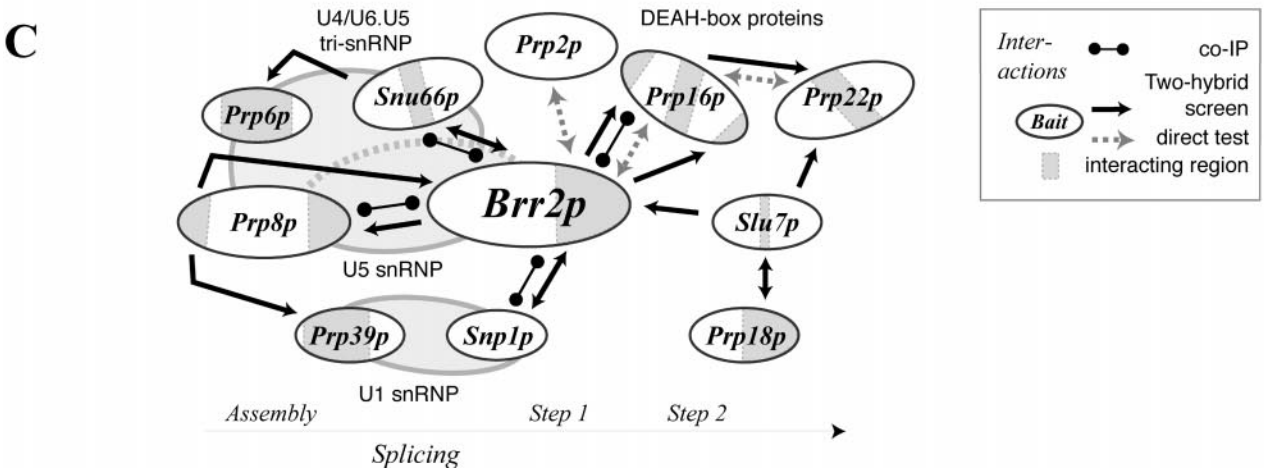

region with the second helicase-like domain was responsible for most Brr2 interactions. Prp2p, nPrp8p, Prp16p, Snu66p, and Slu7p appear to interact differently with the C-terminal Brr2p fragments pulled out in two-hybrid screens (clones B1, B2, and B3). The region that is common to these Brr2p fragments (clone B123) was not sufficient for these interactions, whereas the extreme C terminus by itself interacts strongly with Prp2p, Prp16p, and Snp1p (compare Brr2 clones wild type, ΔM, and C with clone ΔC as bait fusions, and compare Brr2 clones wild type, ΔN, and ΔNΔM with ΔMΔC as prey fusions). In contrast, the interaction with the C-terminal region (clone C or E3) of Prp8p requires the M region of Brr2p (compare Brr2 clones wild type and ΔN with clone ΔNΔM as prey fusions and compare Brr2 clone wild type with clone ΔM as bait fusions). Thus, as for the strength of the interaction (as concluded from the co-immunoprecipitation experiments), the Brr2p region responsible for the interactions with Prp2p, Prp16p, Snp1p, and Snu66p also differs from that responsible for cPrp8p.

Note, in particular, that full-length Prp8p did not show any interactions but that its N terminus and C terminus interacted in a mutually exclusive way with Brr2p: cPrp8p does not interact with truncated Brr2p baits lacking the first helicase domain (*i.e.*, all ΔM variants). In contrast, nPrp8p, like full-length Slu7p, interacted only with such truncated Brr2p fragments (the proline repeats in the extreme N terminus of Prp8p are not required for this interaction). This suggests that different regions of Brr2p interact with the Prp8p termini and also that in spliceosomes particular conformations of either protein might be required for their association. As a summary, the network of splicing protein associations emerging from our protein interaction studies is shown in Figure 5C, indicating how these relate to kinetic events in spliceosome assembly and function.

DISCUSSION

The data presented in this article provide strong evidence for functional interactions between Brr2p (Slt22p/Snu246p/Rss1p/Prp44p) and the splicing factors Prp8p, Prp16p, Snp1p, and Snu66p. Furthermore, we observed other specific two-hybrid interactions that suggest functional links of Brr2p with Slu7p and Prp2p and of Prp16p with Prp22p. Intriguingly, and reminiscent of helicases involved in DNA replication, the interaction of different DExH/DEAD-box proteins might be instrumental during pre-RNA splicing for obtaining specific and optimal unwindase activities. Overall, our data will help to formulate a more accurate model of protein dynamics (and of the central role of Brr2p therein) during spliceosome assembly and subsequent activation of the first and second catalytic steps.

Apart from most Prp8p screens, all two-hybrid screens presented in this article were highly specific and sensitive according to the criteria of Vidal and Legrain (1999). We found interactions with a number of proteins that were previously found as prey of other splicing factors, thus extending the network of protein interactions, identified through two-hybrid screens, that are highly relevant for pre-mRNA splicing (Fromont-Racine *et al.* 1997; Dix *et al.* 1999; Figure 1).

Interactions of Prp8p: Prp8p is a very large protein (280 kD, 2413 amino acids) and different regions have been shown to interact with Snu114p (Dix *et al.* 1998), Snp1p (S. Ruby *et al.*, personal communication), and the yeast homologue of U1C (P. Legrain, personal communication). In a pairwise two-hybrid test, Abovich and Rosbash (1997) found that the N terminus of Prp8p interacted with Prp40p, whereas we found that the Prp8p N terminus associated with Brr2p and Prp39p. Prp8p has been demonstrated to bind to the 5′ splice site region of pre-mRNAs (where U1 snRNPs also associate) in spliceosomes (Teigelkamp *et al.* 1995; Reyes *et al.* 1999), and as the U1 snRNP proteins Snp1p, Prp39p, Prp40p, and yU1C copurify with crude U4/U6.U5 tri-snRNP fractions (Gottschalk *et al.* 1999), their interaction with Prp8p is feasible, even without spliceosomes. Additionally, mutations that affect U4/U6 unwinding in spliceosomes were recently identified in an N-terminal segment of Prp8p (amino acids 193–388; Kuhn and Brow 2000). Thus, taken together, these interactions provide physical evidence to support the proposed role

Figure 5.—Overview of two-hybrid interactions. (A) Fragments of DExH proteins Brr2p, Prp16p, and Prp22p. Prp16p and Prp22p fragments were fished in screens with Brr2p and Slu7p as bait, respectively. Conserved DExH-box regions (GKT, DExH, GRAGR) are indicated as well as the ribosomal protein S1-like RNA-binding region in Prp22p. Prp16p-clone St4 was found in a partial two-hybrid screen with truncated Brr2p lacking the internal 2.5-kb *Bgl*II fragment as bait (Brr2pΔM). For further details see Figure 3A legend. (B) Matrix of interactions between splicing factors in direct Gal4 two-hybrid analysis. The strength of interactions is indicated as resistance to different levels of 3AT (see inset). In the LexA two-hybrid system essentially identical results were obtained (data not shown). Full-length, wild-type Brr2p interacts at 30° (but not at 37°) with full-length Prp2p, Prp16p, Snp1p, and Snu66p. Full-length Prp16p interacts with Brr2p and Prp22p in a temperature-sensitive manner as well. Full-length Prp8p did not interact; only its termini interacted with Brr2p in a mutually exclusive way. See Table 1 for definition of Prp8p, Prp16p, Snp1p, and Snu66p clones. (C) Network of protein interactions during splicing as based on two-hybrid and co-immunoprecipitation analyses described in this article (see inset for details). Snp1p has been reported to retrieve Brr2p in exhaustive two-hybrid screens (Fromont-Racine *et al.* 1997). Arrow at bottom indicates the ordered stages during pre-mRNA splicing.

of Prp8p in the Brr2p-controlled unwinding of U4/U6 and displacement of U1 snRNA from the 5′ splice site, as suggested by genetic data (Kuhn *et al.* 1999).

Recently, genetic analyses and sequence comparisons implicated particular regions of Prp8p in recognizing the uridine tract near the 3′ splice site, in controlling the fidelity of 3′ splice site, selection (Umen and Guthrie 1995a,b, 1996; Collins and Guthrie 1999), in cross-linking to the 5′ splice site (Reyes *et al.* 1999), and in genetic interaction with Prp16p, Prp17p, Prp18p, and Slu7p (Umen and Guthrie 1995b; Ben-Yehuda *et al.* 2000) as well as with the U2 (Xu *et al.* 1998) and U4 snRNAs (Kuhn *et al.* 1999). However, the region of Prp8p that was selected with Brr2p in two-hybrid screens was distinct and more C-terminal to all these regions (prey fusions E3, E4*, and E5*; Figure 3A). In fact, extension of the cPrp8p prey fragment into the upstream segment involved in 3′ splice site interactions abolished the Brr2p interaction (construct E1; Figure 3A). In addition, the upstream segment that inhibited the Brr2p interaction slightly overlaps with part of a region of Prp8p (amino acids 1626–1651) shown by Kuhn and Brow to interact genetically with U4 snRNA (Kuhn and Brow 2000). This is one of two regions of Prp8p proposed by Kuhn and Brow to interact and cause an allosteric change that might initiate spliceosome activation, in part by affecting the activity of Brr2p/Prp44p. As we show here that a distinct, more C-terminal region of Prp8p interacts with Brr2p, conceivably this proposed intramolecular interaction modulates the Prp8p:Brr2p interaction indirectly.

Four further observations support the functional significance of the Prp8p:Brr2p interaction observed here. First, in contrast to regions more upstream, the C terminus of Prp8p implicated in Brr2p interaction is not highly conserved, and when this region of yeast Prp8p was replaced by the plant *Arabidopsis thaliana* counterpart the two-hybrid interaction with Brr2p was lost, and hybrid yeast/plant Prp8p proteins were not functional *in vivo* (J. Hamilton, R. W. van Nues, J. D. Beggs and J. W. S. Brown, unpublished results). Second, in this region the cPrp8p mutation (*prp8-28*) that caused the interaction with Brr2p to be temperature sensitive (Figure 3A) also led to a conditional phenotype *in vivo* (Figure 3B). Third, other mutations, like *prp8-52,* could be isolated that increase the affinity for Brr2p and for the temperature-sensitive slt22-1p (Figure 3A) that has a mutation within the first helicase domain of Brr2p affecting ATP hydrolysis (Xu *et al.* 1996). Mutant prp8-52p, however, did not complement the *slt22-1* allele *in vivo,* presumably because other Brr2p functions that are affected by this allele (Xu *et al.* 1996, 1998) were not suppressed. Fourth, the *prp8-1* allele (which maps to the C-terminal Brr2p-interacting region) was synthetic lethal with *slt22-1* (Figure 3B), whereas no synthetic lethality of *prp8-1* with alleles of other second-step factors has been found (Umen and Guthrie 1995b). The reduced affinity of mutant prp8-1p for Brr2p, as found by two-hybrid analysis (Figure 3A) and co-immunoprecipitation experiments (Figure 4A), could explain the unstable association of prp8-1p with the U5 particle and the diminished assembly of U4/U6.U5 tri-sRNPs observed in heat-treated *prp8-1* extracts (Brown and Beggs 1992).Thus, the strong and specific interaction between Brr2p and the C terminus of Prp8p agrees well with the purification from Hela cells of an RNA-free p220/p200/p116/p40 complex that contains the counterparts of yeast Prp8p, Brr2p, and Snu114p (Achsel *et al.* 1998).

In summary, we propose that the N- and C-terminal regions of Prp8p have distinct interactions that are likely to contribute to the regulation of Brr2p. On the one hand, interaction of nPrp8p with the C terminus of Brr2p may affect the activity of Brr2p in assembling spliceosomes (unwinding the U4/U6 duplex and/or disrupting the U1/5′ splice site interaction), while, on the other hand, interaction of cPrp8p with Brr2p may affect the assembly and/or stability of U5 snRNPs and/or U4/U6.U5 tri-snRNPs. The mutually exclusive nature of these interactions in the two-hybrid assay suggests that Prp8p undergoes conformational rearrangements that could modify the function of Brr2p (and likely other splicing factors also) in the spliceosome.

Interactions of Brr2p: In contrast to Prp8p, screens with the comparably long Brr2p (246 kD; 2163 amino acids) worked well and yielded enough information to delineate interaction domains of Prp8p (as discussed above), Prp16p, and Snu66p. Brr2p, in turn, was fished in screens with nPrp8p (see above), Slu7p, and Snu66p as bait (Figure 1 and Table 1). Apart from interactions with splicing factors, the screens with Brr2p also suggested contacts with proteins involved in other cellular processes such as signal transduction (Fab1p, Cdc25p), cell division (Dbi9p), or gene transcription (Met28p). Although beyond the scope of this article, further analysis of these links might provide insight into the relation between the regulation of the pre-mRNA splicing machinery and that of other cellular events.

Specific association of RNA unwindases: Among the most interesting outcomes of our analyses are the interactions between RNA unwindases; Brr2p with Prp16p and Prp2p on one hand and Prp16p with Prp22p on the other. Because we tested all these proteins against each other using either full-length or truncated forms, we can exclude that these interactions are due to a general stickiness of the conserved helicase domains or that ATP or RNA molecules specifically mediate these interactions (Figure 5 and data not shown). The statistically most relevant two-hybrid interaction of this kind was observed between Brr2p and the N terminus of Prp16p. This interaction, like that between Prp22p and Prp16p (A. Colley and J. D. Beggs, unpublished results), could be reproduced *in vitro* by co-immunoprecipitation assays under nonsplicing conditions. We were

able to pull down Brr2p with nPrp16p without detectable coprecipitation of snRNAs, indicating that no spliceosomal complexes were present and suggesting a direct physical interaction. Both ends of Prp16p that were pulled out as A1 prey of Brr2p are involved in recruitment of Prp16p to the spliceosome (Wang and Guthrie 1998). In contrast, Prp22p needs the internal helicase domain of Prp16p for interaction and acts later in the splicing process (Schwer and Gross 1998), depending on the presence of Prp16p (McPheeters *et al.* 2000). Therefore, our data indicate that Brr2p is the first spliceosomal partner of Prp16p and may act as its receptor in the spliceosome.

The interactions between the four DExH box proteins Brr2p, Prp2p, Prp16p, and Prp22p suggest that during pre-mRNA splicing associations of different unwindases occur, which might be important for their functionality. Interestingly, another DExH-box protein, NS3h from the hepatitis C virus, is active as an (unstable) oligomer (Levin and Patel 1999). NS3h has a helicase domain structure similar to that of bacterial DNA helicases that also function as oligomers (West 1996). Further parallels exist with the proteins of the minichromosome maintenance (MCM) complex that are essential for eukaryotic DNA replication. MCM proteins need to associate to obtain DNA helicase activity (Chong *et al.* 2000), but can also form different complexes with altered functionalities (Lee and Hurwitz 2000), implying different states of the replication machinery or how its action is controlled.

Does the C-terminal helicase-like domain regulate Brr2p function through protein interactions? Our deletion analysis to delineate the protein-binding regions of Brr2p showed that the interaction with the C terminus of Prp8p required the presence of the first helicase domain of Brr2p. In contrast, for all the other interactions analyzed, the C-terminal Brr2p region with the second helicase-like domain was predominantly responsible (Figure 5). This second domain is well conserved between human (Lauber *et al.* 1996), yeast, and plants (GenBank accession no. AC002561) but, in contrast to the first helicase domain, does not seem to be involved in ATP hydrolysis. Mutations in the GKT and DDAH boxes do not cause a phenotype *in vivo* (Kim and Rossi 1999), which further indicates that the protein interactions of this domain, if vital, are not dependent on the altered residues.

Multiple unwindases are implicated in the splicing process (Staley and Guthrie 1998) but little progress has been made in identifying the targets/substrates of their activity. Conceivably, some of these unwindases may work cooperatively on common targets. There is strong evidence that Brr2p recognizes as its substrate not a primary but a particular secondary RNA structure (Lin and Rossi 1996). This secondary structure resembles the U4/U6 snRNA duplex that is unwound by Brr2p (Raghunathan and Guthrie 1998; Kim and Rossi 1999) and the U2/U6 snRNA duplex within which certain U2 snRNA mutants are synthetic lethal with mutations in Brr2p (Xu *et al.* 1996, 1998). It is possible that Brr2p has alternative substrate specificities controlled by its association with different proteins (such as Prp2p or Prp16p) during splicing. Furthermore, in contrast to the transiently associated Prp2p and Prp16p, Brr2p is an integral snRNP protein thought to act at multiple points in the splicing pathway (Staley and Guthrie 1998; see Lauber *et al.* 1996; Xu *et al.* 1996; Raghunathan and Guthrie 1998). If so, multiple interactions will probably contribute to the temporal control of its function. Our data support such a model and suggest that the C-terminal half with the second helicase-like domain might regulate the activity of Brr2p through distinct, sequential protein-protein interactions.

Conclusions: The protein interaction data presented here are compatible with and augment the current model of splicing events (Figure 5C). The strong interaction between Brr2p and the C terminus of Prp8p is important for the assembly and/or stability of the U5 snRNP. Being important for the first step of splicing (Gottschalk *et al.* 1999), Snu66p might facilitate tri-snRNP formation by linking the U5 snRNP and the U4/U6 di-snRNP through its associations with Brr2p and Prp6p. Once the U4/U6.U5 tri-snRNP enters the spliceosome, Snp1p and the N terminus of Prp8p could affect the Snu66p/Brr2p interaction during U1 displacement, with Brr2p being activated to unwind U4/U6 (Kuhn *et al.* 1999). Upon recruitment to the spliceosome Prp2p might redirect the Brr2p activity from the U4/U6 dimer to the U6/U2 snRNA duplex II, which is thought to unwind just before the first catalytic step (discussed in Xu *et al.* 1998). Subsequently, Prp16p could displace Prp2p from Brr2p and induce a conformational change in the spliceosome that exposes the catalytic center to the 3′ splice site. This event further involves Prp8p, Slu7p, and Prp22p (Umen and Guthrie 1995b; Schwer and Gross 1998; McPheeters *et al.* 2000), which might be directly responsible for the release of Prp16p from the 3′ splice site and the spliceosome. The interaction between Prp16p and Brr2p could be weakened upon association of Prp22p with Prp16p and disrupted by Slu7p displacing Prp16p from Brr2p. Experiments to test this proposed order of Brr2p interactions in more detail are beyond the scope of this article, but hopefully we have furthered our understanding of dynamic protein interactions that drive spliceosome function.

We are very grateful to Micheline Fromont-Racine, Jean-Christophe Rain, Pierre Legrain, and other members of the TAPIR network, as well as Dave Brow, Alan Colley, Stephen Dove, John Hamilton, Stephanie Ruby, Paul Smith, and Deming Xu for sharing results before publication. We also thank Deming Xu, Patrizia Fabrizio, Cathy Collins, Stephen Dove, John Hamilton, Denis Lafontaine, Harry Mountain, Jeremy Brown, Hiroyuki Ohkura, Yasuhisu Adachi, Kevin Hardwick, and Joe Lewis for reagents, advice, and strains. Michael Albers, Sarah Johnson, Andrew Fehrenbach, and Nicola Preston deserve big

thanks for their technical support. We thank Andy Newman for constructive comments on the manuscript. This work was supported by the Cancer Research Campaign and program grant no. 047685 from The Wellcome Trust.

LITERATURE CITED

Abovich, N., and M. Rosbash, 1997 Cross-intron bridging interactions in the yeast commitment complex are conserved in mammals. Cell **89:** 403–412.

Achsel, T., K. Ahrens, H. Brahms, S. Teigelkamp and R. Lührmann, 1998 The human U5–220kD protein (hPrp8) forms a stable RNA-free complex with several U5-specific proteins, including an RNA unwindase, a homologue of ribosomal elongation factor EF-2, and a novel WD-40 protein. Mol. Cell. Biol. **18:** 6756–6766.

Ben-Yehuda, S., C. S. Russell, I. Dix, J. D. Beggs and M. Kupiec, 2000 Extensive genetic interactions between *PRP8* and *PRP17/CDC40*, two yeast genes involved in pre-mRNA splicing and cell cycle progression. Genetics **154:** 61–71.

Boronenkov, I. V., J. C. Loijens, M. Umeda and R. A. Anderson, 1998 Phosphoinositide signalling pathways in nuclei are associated with nuclear speckles containing pre-mRNA processing factors. Mol. Biol. Cell **9:** 3547–3560.

Brown, J. D., and J. D. Beggs, 1992 Roles of PRP8 protein in the assembly of splicing complexes. EMBO J. **11:** 3721–3729.

Brys, A., and B. Schwer, 1996 Requirement for SLU7 in yeast pre-mRNA splicing is dictated by the distance between the branchpoint and the 3′ splice site. RNA **2:** 707–717.

Chang, T-H., L. J. Latus, Z. Liu and J. M. Abbott, 1997 Genetic interactions of conserved regions in the DEAD-box protein Prp28p. Nucleic Acids Res. **25:** 5033–5040.

Chong, J. P. J., M. K. Hayashi, M. N. Simon, R-M. Xu and B. Stillman, 2000 A double-hexamer archaeal minichromosome maintenance protein is an ATP-dependent DNA helicase. Proc. Natl. Acad. Sci. USA **97:** 1530–1535.

Collins, C., and C. Guthrie, 1999 Allele-specific genetic interactions between Prp8p and RNA active site residues suggest a function for Prp8p at the catalytic core of the spliceosome. Genes Dev. **13:** 1970–1982.

Dix, I., C. S. Russell, R. T. O'Keefe, A. J. Newman and J. D. Beggs, 1998 Protein-RNA interactions in the U5 snRNP of Saccharomyces cerevisiae. RNA **4:** 1675–1686.

Dix, I., C. S. Russell, S-B. Yehuda, M. Kupiec and J. D. Beggs, 1999 The identification and characterization of a novel splicing protein, Isy1p, of Saccharomyces cerevisiae. RNA **5:** 360–368.

Fabrizio, P., J. L. Laggerbauer, W. S. Lane and R. Lührmann, 1997 An evolutionarily conserved U5 snRNP-specific protein is a GTP-binding factor closely related to the ribosomal translocase EF-2. EMBO J. **16:** 4092–4106.

Fromont-Racine, M., J-C. Rain and P. Legrain, 1997 Toward a functional analysis of the yeast genome through exhaustive two-hybrid screens. Nat. Genet. **16:** 277–282.

Fromont-Racine, M., A. E. Mayes, A. Brunet-Simon, J.-C. Rain, A. Colley *et al.*, 2000 Genome-wide yeast protein interaction screens reveal functional networks involving Sm-like proteins. Yeast **17:** 95–110.

Gottschalk, A., G. Neubauer, J. Banroques, M. Mann, R. Lührmann *et al.*, 1999 Identification by mass spectrometry and functional analysis of novel proteins of the yeast [U4/U6.U5] tri-snRNP. EMBO J. **18:** 4535–4548.

Hodges, P. E, S. P. Jackson, J. D. Brown and J. D. Beggs, 1995 Extraordinary sequence conservation of the PRP8 splicing factor. Yeast **11:** 337–342.

Ishikawa, S., M. Kai, M. Tamari, Y. Takei, K. Takeuchi *et al.*, 1997 Sequence analysis of a 685-kb genomic region on chromosome 3p22-p21.3 that is homozygously deleted in a lung carcinoma cell line. DNA Res. **4:** 35–43.

Jackson, S. P., M. Lossky and J. D. Beggs, 1988 Cloning of the RNA8 gene of Saccharomyces cerevisiae, detection of the RNA8 protein, and demonstration that it is essential for nuclear pre-mRNA splicing. Mol. Cell. Biol. **8:** 1067–1075.

Kikuchi, M., M. Nakao, Y. Inoue, K. Matsunaga, S. Shichijo *et al.*, 1999 Identification of a SART-1-derived peptide capable of inducing HLA-A24-restricted and tumor-specific cytotoxic T lymphocytes. Int. J. Cancer **81:** 459–466.

Kim, S. H., and R. J. Lin, 1996 Spliceosome activation by PRP2 ATPase prior to the first transesterification reaction of pre-mRNA splicing. Mol. Cell. Biol. **16:** 6810–6819.

Kim, D. H., and J. J. Rossi, 1999 The first ATPase domain of the yeast 246-kDa protein is required for *in vivo* unwinding of the U4/U6 duplex. RNA **5:** 959–971.

Kuhn, A. N., and D. A. Brow, 2000 Suppressors of a cold-sensitive mutation in yeast U4 RNA define five domains in the splicing factor Prp8 that influence spliceosome activation. Genetics **155:** 1667–1682.

Kuhn, A. N., Z. Li and D. A. Brow, 1999 Splicing factor Prp8 governs U4/U6 RNA unwinding during activation of the spliceosome. Mol. Cell **3:** 65–75.

Lauber, J., P. Fabrizio, S. Teigelkamp, W. S. Lane, E. Hartmann *et al.*, 1996 The HeLa 200kDa U5 snRNP-specific protein and its homologue in Saccharomyces cerevisiae are members of the DEXH-box protein family of putative RNA helicases. EMBO J. **15:** 4001–4015.

Lee, J-K., and J. Hurwitz, 2000 Isolation and characterization of various complexes of the minichromosome maintenance proteins of *Schizosaccharomyces pombe*. J. Biol. Chem. **275:** 18871–18878.

Levin, M. K., and S. S. Patel, 1999 The helicase from hepatitis C virus is active as an oligomer. J. Biol. Chem. **274:** 31839–31846.

Lin, J., and J. J. Rossi, 1996 Identification and characterization of yeast mutants that overcome an experimentally introduced block to splicing at the 3′ splice site. RNA **2:** 835–848.

Mayes, A. E., L. Verdone, P. Legrain and J. D. Beggs, 1999 Characterization of Sm-like proteins in yeast and their association with U6 snRNA. EMBO J. **18:** 4321–4331.

McPheeters, D. S., B. Schwer and P. Muhlenkamp, 2000 Interaction of the yeast DExH-box RNA helicase Prp22p with the 3′ splice site during the second step of nuclear pre-mRNA splicing. Nucleic Acids Res. **28:** 1313–1321.

Mortillaro, M. J., and R. Berezney, 1998 Matrin CYP, an SR-rich cyclophilin that associates with the nuclear matrix and splicing factors. J. Biol. Chem. **273:** 8183–8192.

Mountain, H. A., A. S. Bystrom, J. T. Larsen and C. Korch, 1991 Four major transcriptional responses in the methionine/threonine biosynthetic pathway of Saccharomyces cerevisiae. Yeast **8:** 781–803.

Newman, A. J., and C. Norman, 1992 U5 snRNA interacts with exon sequences at 5′ and 3′ splice sites. Cell **68:** 743–754.

Newman, A. J., S. Teigelkamp and J. D. Beggs, 1995 snRNA interactions at 5′ and 3′ splice sites monitored by photoactivated cross-linking in yeast spliceosomes. RNA **1:** 968–980.

Noble, S. M., and C. Guthrie, 1996 Identification of novel genes required for yeast pre-mRNA splicing by means of cold-sensitive mutations. Genetics **143:** 67–80.

O'Keefe, R. T., and A. J. Newman, 1998 Functional analysis of the U5 snRNA loop 1 in the second catalytic step of yeast pre-mRNA splicing. EMBO J. **17:** 565–574.

Parchaliuk, D. L., R. D. Kirkpatrick, R. Agatep, S. L. Simon and R. D. Gietz, 1999 Yeast two-hybrid system screening. Technical Tips Online (http://tto.trends.com).

Raghunathan, P. L., and C. Guthrie, 1998 RNA unwinding in U4/U6 snRNPs requires ATP hydrolysis and DEIH-box splicing factor Brr2. Curr. Biol. **8:** 847–855.

Rain, J-C., and P. Legrain, 1997 *In vivo* commitment to splicing in yeast involves the nucleotide upstream from the branch site conserved sequence and the Mud2 protein. EMBO J. **16:** 1759–1771.

Reyes, J. L., E. H. Gustafson, H. R . Luo, M. J. Moore and M. M. Konarska, 1999 The C-terminal region of hPrp8 interacts with the conserved GU dinucleotide at the 5′ splice site. RNA **5:** 167–179.

Saiz, J. E., M. A. Santos, C. R. Vazquez de Aldana and J. L. Revuelta, 1999 Disruption of six unknown open reading frames from Saccharomyces cerevisiae reveals two genes involved in vacuolar morphogenesis and one gene required for sporulation. Yeast **15:** 155–164.

Schwer, B., and C. H. Gross, 1998 Prp22, a DExH box RNA helicase, plays two distinct roles in yeast pre-mRNA splicing. EMBO J. **17:** 2086–2094.

Staley, J. P., and C. Guthrie, 1998 Mechanical devices of the spliceosome: motors, clocks, springs, and things. Cell **92:** 315–326.

Staley, J. P., and C. Guthrie, 1999 An RNA switch at the 5′splice site requires ATP and the DEAD box protein Prp28p. Mol. Cell **3:** 55–64.

Stevens, S. W., and J. Abelson, 1999 Purification of the yeast U4/U6.U5 small nuclear ribonucleoprotein particle and identification of its proteins. Proc. Natl. Acad. Sci. USA **96:** 7226–7231.

Su, Y. A., M. M. Lee, C. M. Hutter and P. S. Meltzer, 1997 Characterization of a highly conserved gene (OS4) amplified with CDK4 in human carcinoma's. Oncogene **15:** 1289–1294.

Teigelkamp, S., A. J. Newman and J. D. Beggs, 1995 Extensive interactions of PRP8 protein with the 5′ and 3′splice sites during splicing suggest a role in stabilization of exon alignment by U5 snRNA. EMBO J. **14:** 2602–2612.

Umen, J. G., and C. Guthrie, 1995a A novel role for a U5 snRNP protein in 3′ splice site selection. Genes Dev. **9:** 855–868.

Umen, J. G., and C. Guthrie, 1995b Prp16p, Slu7p, and Prp8p interact with the 3′ splice site in two distinct stages during the second catalytic step of pre-mRNA splicing. RNA **1:** 584–597.

Umen, J. G., and C. Guthrie, 1996 Mutagenesis of the yeast gene PRP8 reveals domains governing the specificity and fidelity of 3′ splice site selection. Genetics **143:** 723–739.

Vidal, M., and P. Legrain, 1999 Yeast forward and reverse 'n'-hybrid systems. Nucleic Acids Res. **27:** 919–929.

Vidal, V. P. I., L. Verdone, A. E. Mayes and J. D. Beggs, 1999 Characterization of U6 snRNA-protein interactions. RNA **5:** 1470–1481.

Wagner, J. D. O., E. Jankowsky, M. Company, A. M. Pyle and J. N. Abelson, 1998 The DEAH-box protein PRP22 is an ATPase that mediates ATP-dependent mRNA release from the spliceosome and unwinds RNA duplexes. EMBO J. **17:** 2926–2937.

Wang, Y., and C. Guthrie, 1998 PRP16, a DEAH-box RNA helicase, is recruited to the spliceosome primarily via its nonconserved N-terminal domain. RNA **4:** 1216–1229.

Wang, Y., J. D. O. Wagner and C. Guthrie, 1998 The DEAH-box splicing factor Prp16 unwinds RNA duplexes *in vitro*. Curr. Biol. **8:** 441–451.

West, S. C., 1996 DNA helicases: new breeds of translocating motors and molecular pumps. Cell **86:** 177–180.

Wishart, M. J., and J. E. Dixon, 1998 Gathering STYX: phosphatase-like form predicts functions for unique protein-interaction domains. Trends Biochem. Sci. **23:** 301–306.

Xu, D., S. Nouraini, D. J. Field, S-J. Tang and J. D. Friesen, 1996 An RNA-dependent ATPase associated with U2/U6 snRNAs in pre-mRNA splicing. Nature **381:** 709–713.

Xu, D., D. J. Field, S-J. Tang, A. Moris, B. P. Bobechko *et al.*, 1998 Synthetic lethality of yeast slt mutations with U2 small nuclear RNA mutations suggests functional interactions between U2 and U5 snRNPs that are important for both steps of pre-mRNA splicing. Mol. Cell. Biol. **18:** 2055–2066.

Zhang, X., and B. Schwer, 1997 Functional and physical interaction between the yeast splicing factors Slu7 and Prp18. Nucleic Acids Res. **25:** 2146–2152.

Communicating editor: F. Winston